2D AND 3D MODELLING OF PTEROSAUR WING AERODYNAMICS

Abstract

An overview of the research on the morphology of pterosaurs demonstrates a unique flying vertebrate, anatomically designed for manoeuvrability in flight. It is considered that the pteroid bone played an important role in flight dynamics. Results from wind tunnel tests have shown improvement in lift performance resulting from an extended front wing flap (the propatagium) which was supported and adjusted in width and angle by the changes in orientation of the pteroid bone. In this paper, 2d modelling will be examined and used as comparison for the wind tunnel results. 3d modelling will be demonstrated and implications discussed.

Background

Pterosaurs were the first vertebrates to evolve powered flight and Martill (2003) remarks that they flew 'really rather elegantly'. Their name is of Greek origin and means Winged Lizards. These proficient fliers ruled the skies for over 140 million years from the late Triassic period until they became extinct at the end of the Cretaceous period. There were more than 120 species ranging from the size of a small sparrow to later species with wing spans of over 10 meters. A highly successful group named Azhdarchids after of Uzbek mythical dragon, achieved wing spans comparable with light aircraft (Witton 2007). It is thought by several researchers that evolving trends in higher wind speeds may have been incompatible with their aerodynamic function and thus heralded their extinction.

Although there are scant fossil remains of the wing membrane, Martill 2003 says that they were extraordinarily light and beautifully engineered. Unwin 2003 cites evidence of a wing membrane structure just 0.5mm thick. These remains show a vast number of actinofibrils orientated like the main structural elements in wings of birds, providing stiffness and integrity and possibly surface curvature for aerodynamic efficiency. These complex wing membranes also comprise of muscle fibres, blood vessels and sensory nerves which Unwin terms 'Smart Wings' in view of further evidence to support extensive neural coordination.

Witmer et al 2003 constructed digital endocasts of two pterosaur brain and vestibular apparatus from computed tomographic (CT) scans. These showed that the area occupied by the semi-circular canal was relatively twice that found in birds. Birds have a larger labyrinth compared to mammals which is associated with equilibrium and flight control. They also found that the pterosaurs flocculi occupied a massive 7.5% of total brain mass, in birds this is only between 1 and 2%. The flocculus is a region of the brain that integrates signals from joints, muscles, skin and balance organs. These factors suggest that pterosaurs possessed superior equilibrium and high level processing of

extensive sensory information from the wing membrane, joints and sensory organs.   This would have provided the potential for fine tuning their flight manoeuvres.

Birds also have tail feathers which they use like a rudder to aid control of flight direction, lift and drag.   Although pterosaurs lacked this tail control, some species possessed large head crests which may have acted like a fin to aid yaw.   Some authors however, consider that these head crests may have hindered flight and were perhaps only of significance in mating. The possibility that some pterosaur species had hair like structures would indicate that they were endothermic, another factor which would assist in powered flight.

Wilkinson (2005) provides a clear diagram of wing orientation with the main wing or cheiropatagium stretched between fore and hind limbs providing a large sail like surface area. A smaller crescent shaped (cruropatagium) membrane attached to the medial aspect of the hind limbs and was controlled by the fifth toe Unwin and Bakhurina 2002. The propatagium spanned in front of the arm from the shoulder to the distal end of the medial carpal. The angle of attack of this forewing could be adjusted by a supporting bone, the pteroid, which after microscopic analysis, Unwin et al (1996) conclude is a true bone that articulated at the wrist.   (Fig 1)
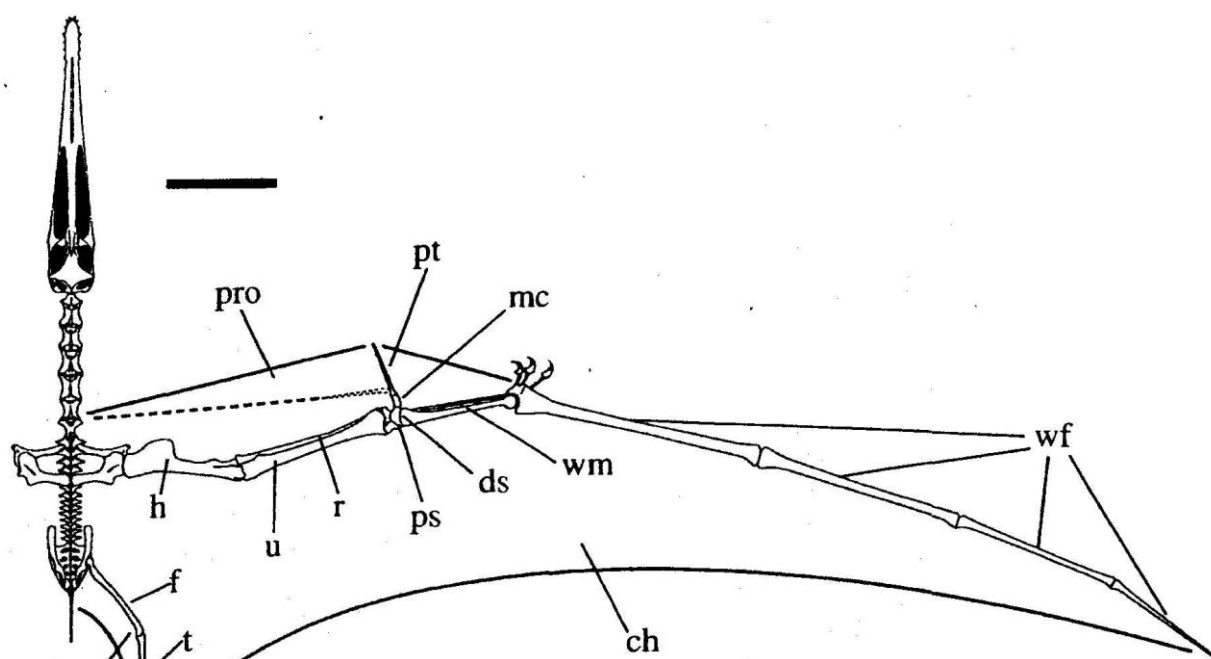

Figure 1 – Reconstructed skeleton of the right wing of A. santanae in dorsal view Wilkinson et al (2005), adapted from Wellnhofer (1991b). It shows the pteroid extending forward supporting a broad propatagium (solid line) and flexed medially with the pteroid forming part of the leading edge (broken line): scale bar 200mm. Abbreviations: ch, cheiropatagium; cr, cruropatagium; ds distal syncarpal; f, femur; h, humerus; mc, medial carpal; pro, propatagium; ps, proximal syncarpal; pt, pteroid; r, radius; t tibiotarsus; u, ulnar; wf, wing finger; wm, wing metacarpal.

Fossil evidence of pteranodon ingens was examined by Bramwell and Whitfield (1974). They found that the bones contained air sacs and the thickness of bone walls was between 0.5 and 1.3mm. Fig 2 shows a cross section of the sub-triangular first phalanx (BM no 41637) and a metacarpal (B.M. no 39417). Here the bone wall is thickest at each angle to confer strength. This pneumatic bone structure provided low mass relative to large wing area resulting in low wing loading. They estimated an 18.1kg mass for a pteranodon with a wing span of 8.2m which is consistent with later estimations. See appendix ii) for comparison between pterosaur and avian bone structure.
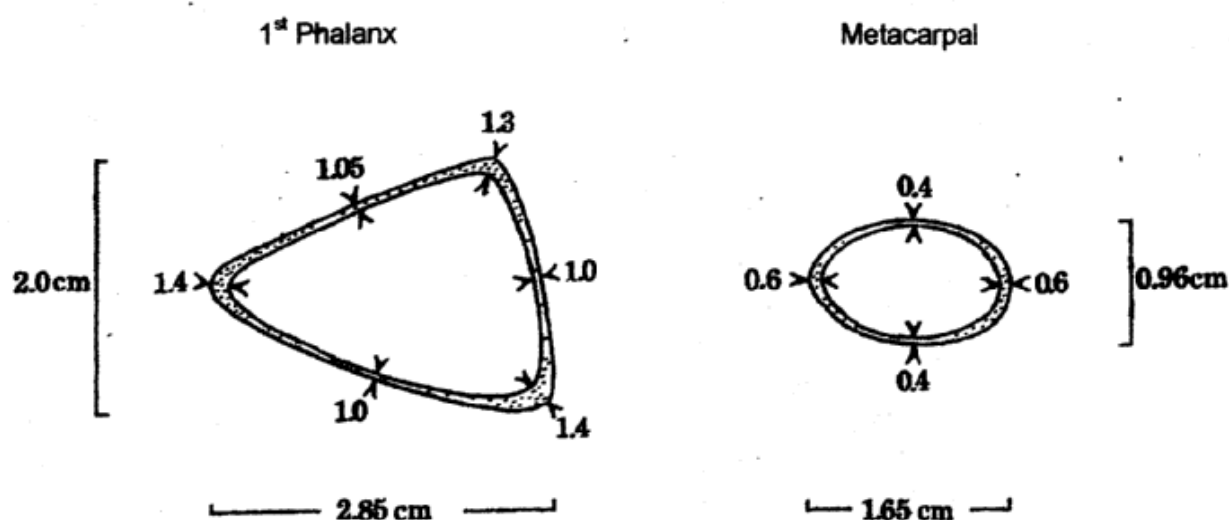

| 1st Phalanx | Metacarpal |

Figure 2 – Cross-section of a first phalanx (B.M. no 41637) and a Metacarpal (B.M. no 39417). Thickness of bone measured in millimetres. Bramwell and Whitfield (1974)

The fact that pterosaur skeletal structure was hollow and therefore fragile, poses questions relating to land locomotion. Martill and Unwin (1989) examined evidence from Lower Cretaceous pterosaur wing membranes from Brazil. It showed that the proximal region of the cheiropatagium lacked fibres, was thin and wrinkled and attached to the hind limb. This would support hypothesis that the wing finger folded back to enable a quadruped stance. (Fig 3)

So how did they take off? Some authors described them on all fours 'scrabbling' to the edge of cliff tops. Or rearing up on hind legs for a running take off Stein (1975). Others consider that they would simply be able to face an oncoming breeze with their wings raised to achieve flight Bramwell and Whitfield (1974).
Once in flight minimal flapping would be required with possible manageability from the wing structure which would be built for gliding not for continual flapping

flight as shown by the hollow bone structure in figure 2 in contrast to a humming bird bone structure.

Figure 3 – A. Santanae from Wellnhofer (1991b)

In fossil lie, the pteroid bone has been discovered pointing towards the shoulder. It was thought by researchers that it formed part of the leading edge of the propotagium and therefore considered fairly insignificant in the overall mechanics of pterosaur flight. However, Frey and Riess 1981 examined evidence to support a greater range of movement of the pteroid. They believed that it could extend forward and downward to broaden the forewing and increase wing camber. With the ability to move in a vertical plane, the pteroid would have adjusted the propatagium like a forward wing flap. In view of the pneumatic nature of the pteroid in some species of pterosaur and its long thin shape, some researchers argued that it would have been too fragile to withstand leading edge forces. Further analysis of exceptionally well preserved fossils from the Santana Formation in Brazil, shows compelling evidence to support a forward, downward and medial articulation of the pteroid. Fig 4
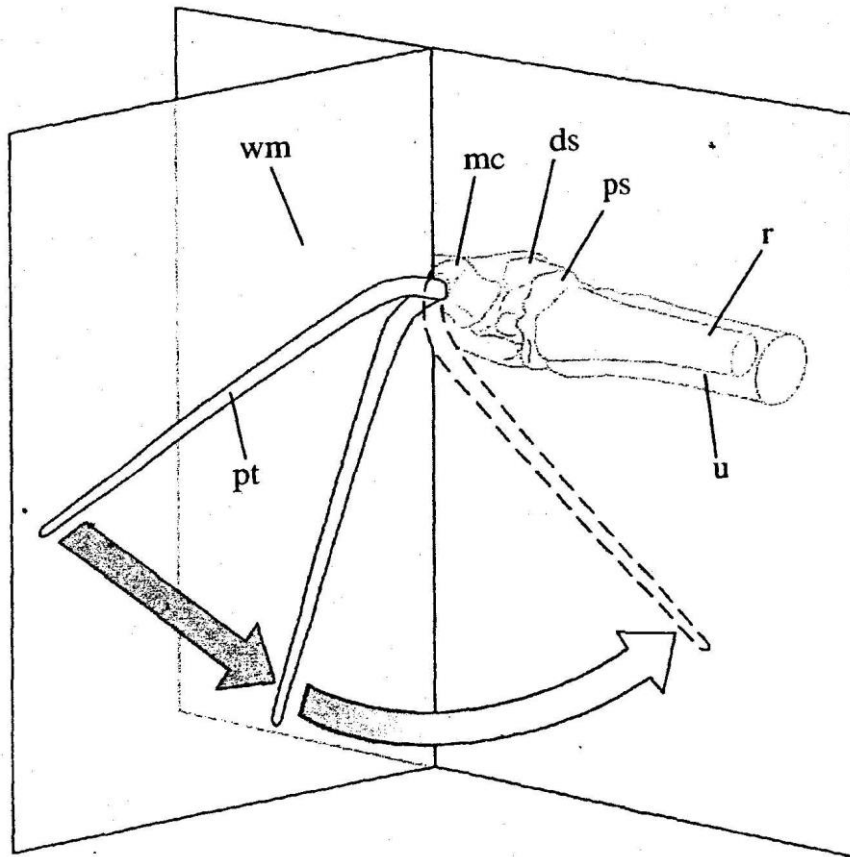
Figure 4 – Right wrist in antero-medial view, showing articular motion of the pteroid. Two planes have been superimposed, intersecting at the carpal-pteroid joint, one parallel to the wing spar and one normal to it. Initial flexion draws the pteroid downward and it remains in the normal plane. The pteroid then rotates laterally towards the parallel plane as shown by the broken line. Abreviations:
Ds, distal syncarpal; mc, medial carpal; ps, proximal syncarpal; pt, pteroid; r, radius; u, ulnar; wm, wing metacarpal. (Wilkinson et al 2005)

In an attempt to validate theories regarding the function of the pteroid bone, Wilkinson et al (2005) carried out wind tunnel tests. They constructed three different wing models using aluminium tube for the arm and steel wire to support a non-elastic nylon fabric:

1. With the pteroid extended forward and a broad propatagium
2. With the pteroid flexed medially and a narrow propatagium
3. With no pteroid or propatagium

Their results showed that a broad propatagium with the pteroid pointing antero-ventrally performed better than a narrow propatagium with the pteroid pointing medially toward the shoulder. Performance was best with the propatagium deflected between 30° and 40° and with an angle of attack between 2° – 16°

degrees. At lower angles of attack performance was best with a deflection of less than 30 degrees as greater deflection was found to obstruct air flow.

The aim of this investigation is to provide results which support Wilkinson's physical models showing the high lift characteristics using the same Reynolds number and subsequently changing the parameters indicative to the result. Suitably researched parameters will be used to generate the models.

2D AND 3D METHODOLOGY

Comparing physical and computational results

In order to analysis the desirable characteristics of the wing orientations the Lift Drag ratio's will be plotted. Fluent will give out the lift and drag forces to be calculated in a spreadsheet using the coefficient formulae below for lift and drag. Since Fluent is unsuitable for outputting the coefficient, this will be calculated manually.

$$C_L = \frac{2L}{\rho \bullet V^2 \bullet A} \qquad (1)$$

$$C_D = \frac{2D}{\rho \bullet V^2 \bullet A} \qquad (2)$$

Figure 5 shows a Gambit wing profile model constructed with NURBS (Non-uniform Rational Bezier Spline) in order to make sure the camber was a smooth curve. The leading edge or propatagium is to the left of the round spar. The propatagium deflection angle ($\emptyset$pd) is varied to emulate the movement of the pteroid bone. Increasing the $\emptyset$pd, increases deflection of the propatagium also increasing the profile area. To the right of the spar is the curved main wing or cheiropatagium.
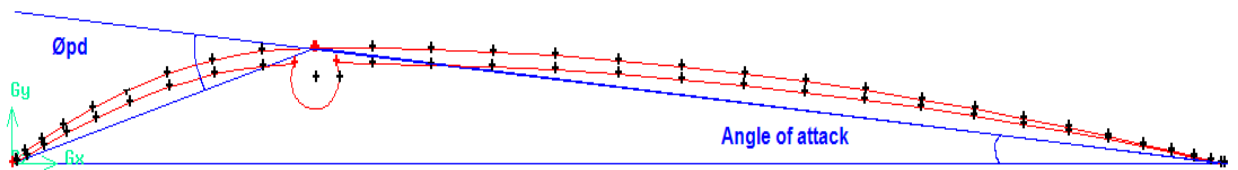
Figure 5 – Gambit diagram of wing profile model 32° propatagium deflection at a 5° angle of attack

The aerodynamics of a creature's wing is comparable to an aerofoil, as they are both analysed using the lift drag coefficient ratio. The first progression in this investigation was to compare Java Foil, a program specialised in aerofoil analysis, with the familiar Computation Fluid Dynamics (CFD) program solver Fluent.
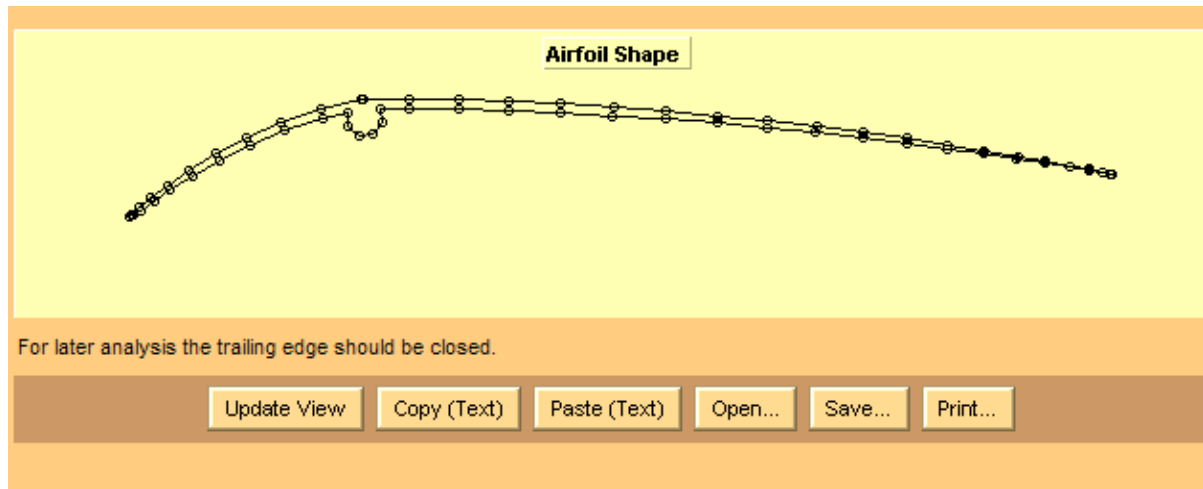
Figure 6 – Java foil Screen shot of modified wing profile with front edge flap at 32°.

Java Foil is designed to analyse 2d aerofoil configurations, it is available free online and is programmed with C++ to calculate fluid flow using potential flow. This method of calculation could be considered dated in comparison to the more up to date methods of CFD using control volumes with meshing covering the calculated area. The meshing density used in CFD must be higher with areas of interest such as the boundary layer. Here it is important to have a cell volume size smaller than the thickness of the examined boundary layer surrounding the aerofoil. This is true particularly for the leading and trailing edges to examine vortices shedding. The solver Fluent implements the control volume method with a mesh file which can be made in pre-program Gambit (modelling program). The process of creating the same shape model for comparison was speeded up by importing an ICEM file which is a notepad file with the 3d co-ordinates saved as a .dat file, which can then be read by the modelling program Gambit.

The models will also be analysed by Java Foil for comparison. Unlike Fluent, Java Foil does not need a specified inlet velocity, as a Reynolds number is applied. The Reynolds number was set to 1.2×10^{5} for comparison to the physical model run by Wilkinson. For the comparison in Java Foil the spar diameter had to be added with extra co-ordinates generated in Gambit by splitting the edges. These extra co-ordinates were unnecessary in Gambit as shown in figure 5 as the round spar was generated in Gambit by three vertices, the centre and two points with the same radius from the centre.

With the turbulent flow occurring at a Reynold's number of 2300, it was clear that the flow would be modelled best with a viscous turbulent model. K-epsilon and K-omega were tested and contrasted. These two models each use 2 equations to calculate the viscous model. Although results between K-epsilon and K-omega were similar, the latter showed higher and lower extremes. This therefore was the chosen viscous model as it was felt this would highlight any changes in flight characteristics.

The models analysed in Fluent and Java Foil had a curved camber of 7 to simulate the slackness of the membrane elasticity. The camber was generated in Java Foil and imported into Fluent though Gambit. The trailing edge was set with a chord length of 0.753741m and an arc length of 0.754960m. The maximum angle of attack for the models was dictated by angles that would not cause tail strike during landing. Tail strike is a term used to describe the trailing edge of a plane touching the ground as it is landing.

Each orientation of the wing was generated as a mesh file of around 40,000 cells with concentrated mesh interval size of 0.02m for a chord length of 1m. The sides surrounding the control volume were meshed with 0.5m interval size.
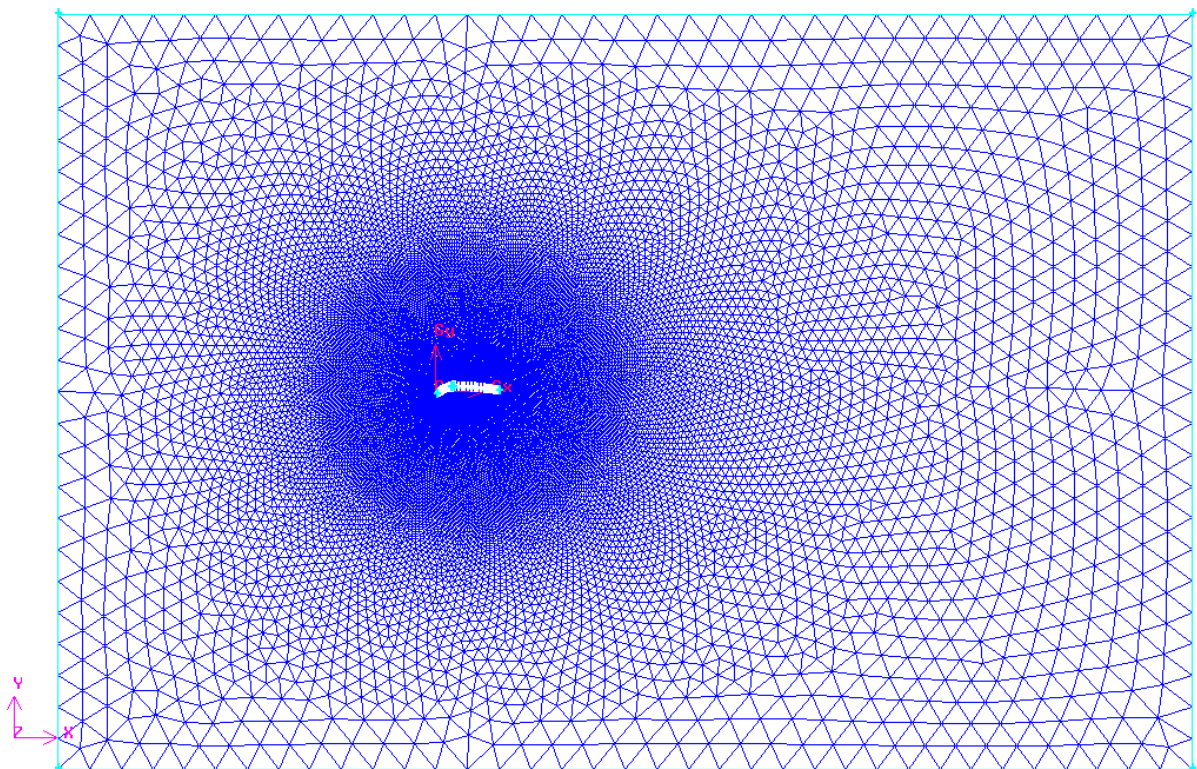
Figure 7 – Gambit mesh for 32° ∅pd

The boundary conditions applied include the inlet velocity on the left side and pressure outlet on the opposite side of the control volume. The top and bottom are under symmetry conditions. The shape and size of the control volume was tested for analysis of lift without hindrance from swirl anomalies. This unwanted swirling occurred with a semi circular inlet. The simple rectangular control volume with symmetry conditions best simulates the turbulent model without interference. The interval count was also sufficient to the show the boundary layer as the cell volumes are smaller than the boundary layer.

Judging from fossil evidence the total weight of a sub adult pterosaur using a safe over estimate would be 12kg.

The 2d models were constructed from the cross section of the 3d model generated. A model 3d model was created to get to grips with the shape and overall structure.

Both 2d and 3d models were analysed in order to look at any similarities to previous research, such as Wilkinson and Unwin. The nylon wing membrane of the physical model in Wilkinson's research was tensioned appropriately to mimic the fibrous membrane. However, with only scant fossil remains of soft tissue it is impossible to be certain about the true elastic property and behaviour of the wing membrane.

Wilkinson's study provided them with suitable results to suggest that the pteroid bone was positioned antero-ventrally in flight and that it could be adjusted to aid manoeuvrability. Bramwell and Whitfield (1974) also agree that movement of the pteroid altered the angle and shape of the propatagium to aid flight. In fossils the pteroid was found orientated medially and many researches previously theorized that its sole purpose was to act as a leading edge for the propatagium. However evidence from well preserved soft tissue wing membrane Martill and Unwill (1989) and areas of muscle attachment on skeletal remains have provided a greater understanding of the flight mechanics of these creatures, to support the dynamic nature of wing adjustment.

In gliding the pterosaur locked its bones into place evidence of this is shown in notches in the shoulder joints Bramwell and Whitfield (1974). The in-flight phase would then involve minimal flapping, mainly using the wing membranes for lift eg. sea lift and thermals. There is evidence to show that pterosaurs inhabited costal, lagoon and waterway areas. Taking off is thought to have involved hanging like bats off the nearest cliff edge. The membranous wings produce more stability than hard aerofoils. This provides suitable evidence that pterosaur manoeuvrability was a direct result of the pteroid adjusting the propatagium, a biological front aileron. The f16 is designed with front flaps or aileron with an attempt to maximise agility.

It took in excess of 200 hours in order to attain aesthetic likeness in a 3d computer model with maximum accuracy. After trying to use a familiar engineering modelling tool Solid Works it became apparent that it did not have a high enough flexibility in editing shapes such as a pterosaur wing. The next software looked at was Studio Max which is a similar software to that used to model the animations in Jurassic Park. After taking time to learn how to use this program it was then possible to proceed. A scaled drawing was sourced from Wilkinson et al (2005). This was then scanned into Studio Max which allowed reference drawings to line up appropriately. A skeletal structure was created and a covering was attached to represent the fibrous membrane. The area of interest was the wing and the orientation of the pteroid bone. Studio Max allows bone like assemblies to be created and modified suitably allowing interaction, enabling orientation and if desired, animation.
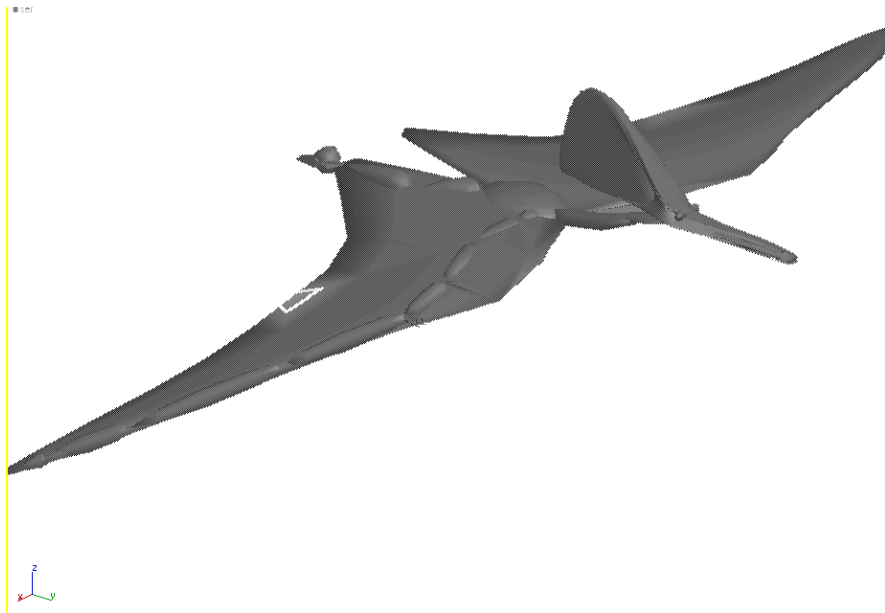
Figure 8 – 3d Studio Max model Pterosaur in flight

Gambit enables the user to rotate the selected edges and this was how the varied wing profiles were generated. **The same is possible in Studio Max but bone structure and skin movement can be linked with motile forces from muscles.** While the models were generated in 2d for analysis, the 3d model also helped to visualise the change in shape of the wing profile in a 3d sense.
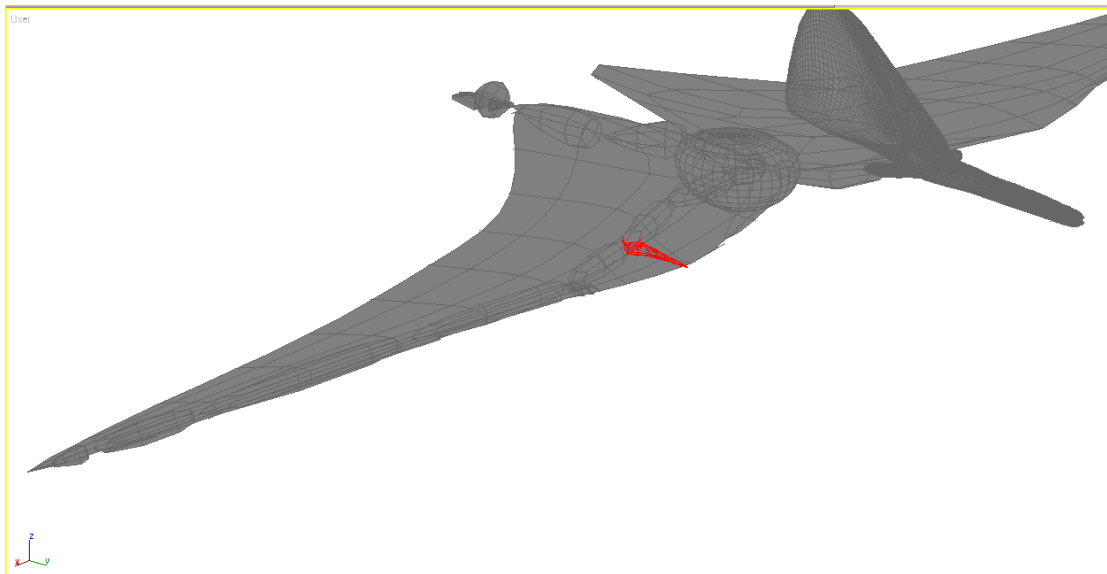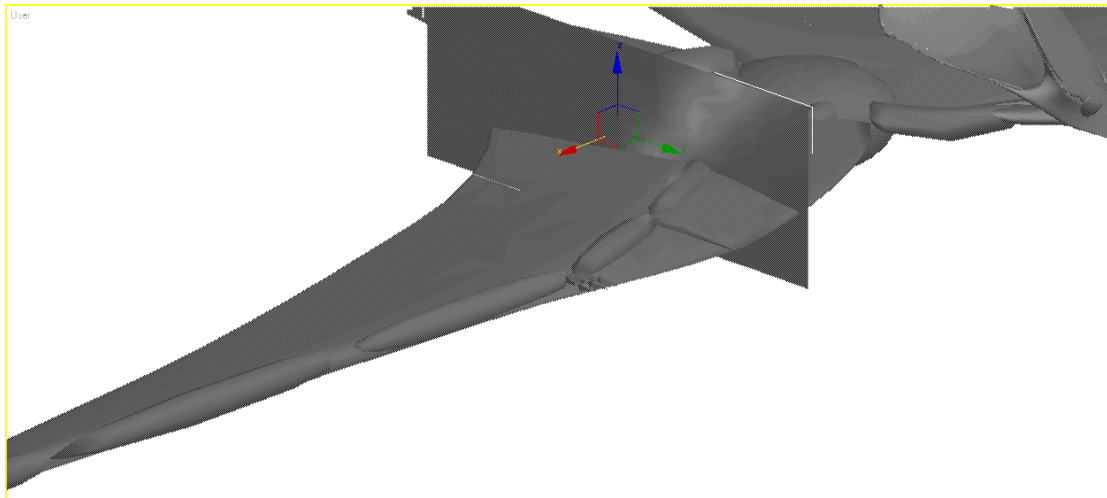

Figure 9 – Wire frame with highlighted pteroid bone
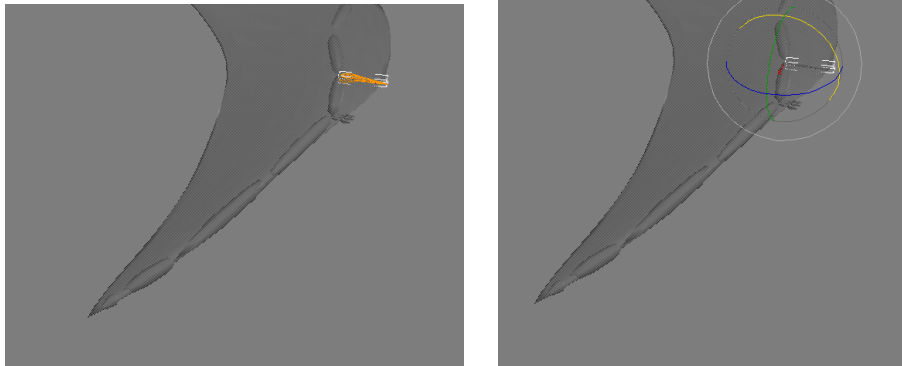
Figure 10 – Studio Max images showing changing orientation of pteroid bone

The orientation of the pteroid bone was adjusted to the angle with the maximum lift. Converting the model from studio max to a 2d profile created a varying shape as the pteroid bone was tensioned.

Figure 11 – Highlighted plane showing were 2d cross section was taken.

For use of Java Foil to provide comparison to the Gambit models, the modified leading edge angle coordinates were input in the freeware software and this was updated into Java Foil's wing profile. In an attempt to keep the same level of accuracy by using the same number vertices to outline the wing profile, 61 points were used. Any lower than 50 points and inaccuracies would occur from over simplification. Modifying the front edge flap required changing about 25 vertices on every profile model.
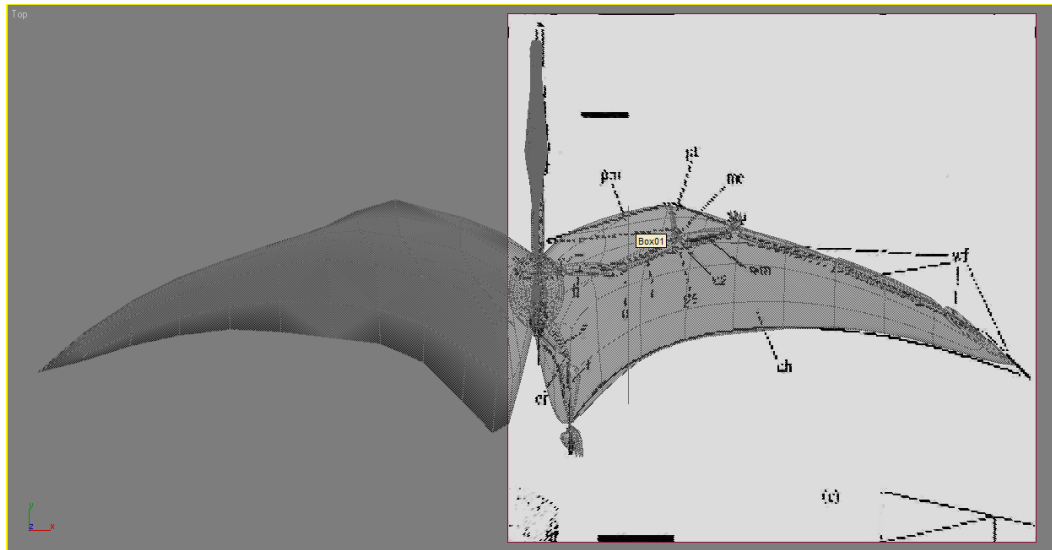
Figure 12 – Showing construction of 3d model using figure 1 as template.

Figure 12 shows the final method of construction using the scaled template in Studio Max. This allows the transparent wire frame outline to be aligned with figure 1, a scaled adapted from A.Santanae pterosaur in Wilkinson (2005). Note the realistic curvature of tissues mirrored on the left hand side.
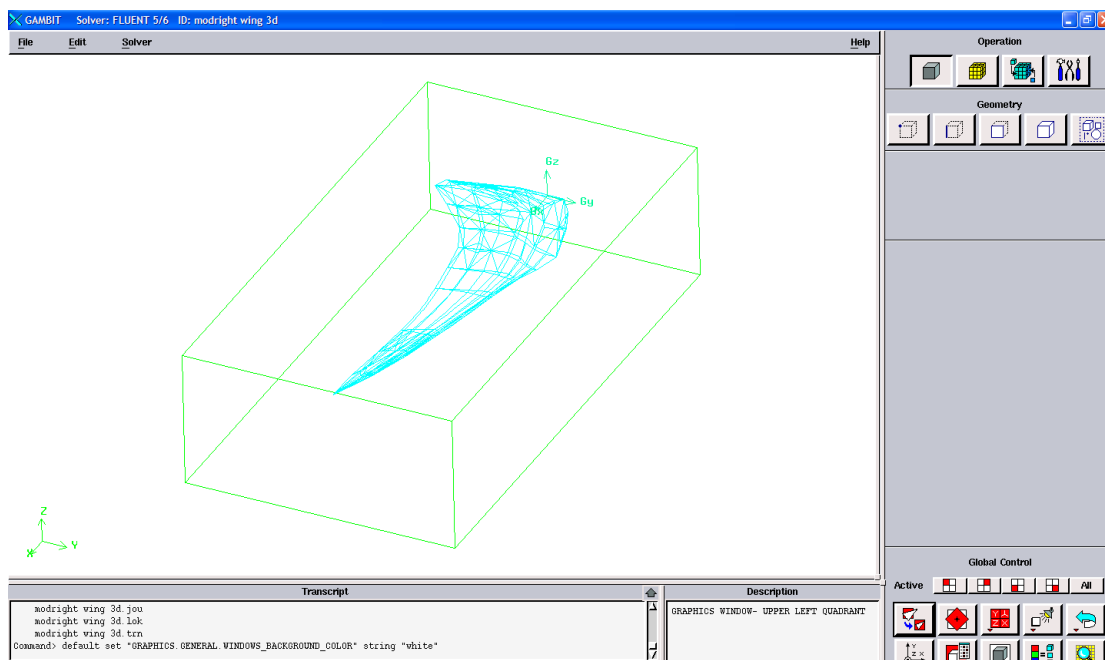

Figure 13 – Imported 3d Gambit model.

The model in Figure 13 required changes in tolerances for faces to be connected. The 2d modelling was sufficient to show the high lift function of a front flap at high angles of attack, 3d models were demonstrated but not used for comparison. Methods for analysis in 3d Fluent were learnt though trial and error. It is thought that the 3d shape would have an overall effect on the drag.

K-epsilon required approximately 60,000 iterations; this is 15 times the amount required for the viscous model Omega and therefore took far more time. All the models were at two different Reynolds numbers i.e. two different inlet velocities. This aided the comparison between Fluent and Java Foil in analysis.

2D RESULTS
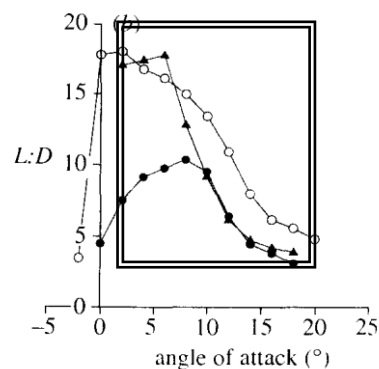
Figure 14 - Showing Wilkinson's results with area's modelled in frame

Figure 15 encompasses the wing orientations from the framed section in figure 14. Areas of interest were sampled at more frequent angles of attack in order to show the change flight characteristics at 2° intervals.
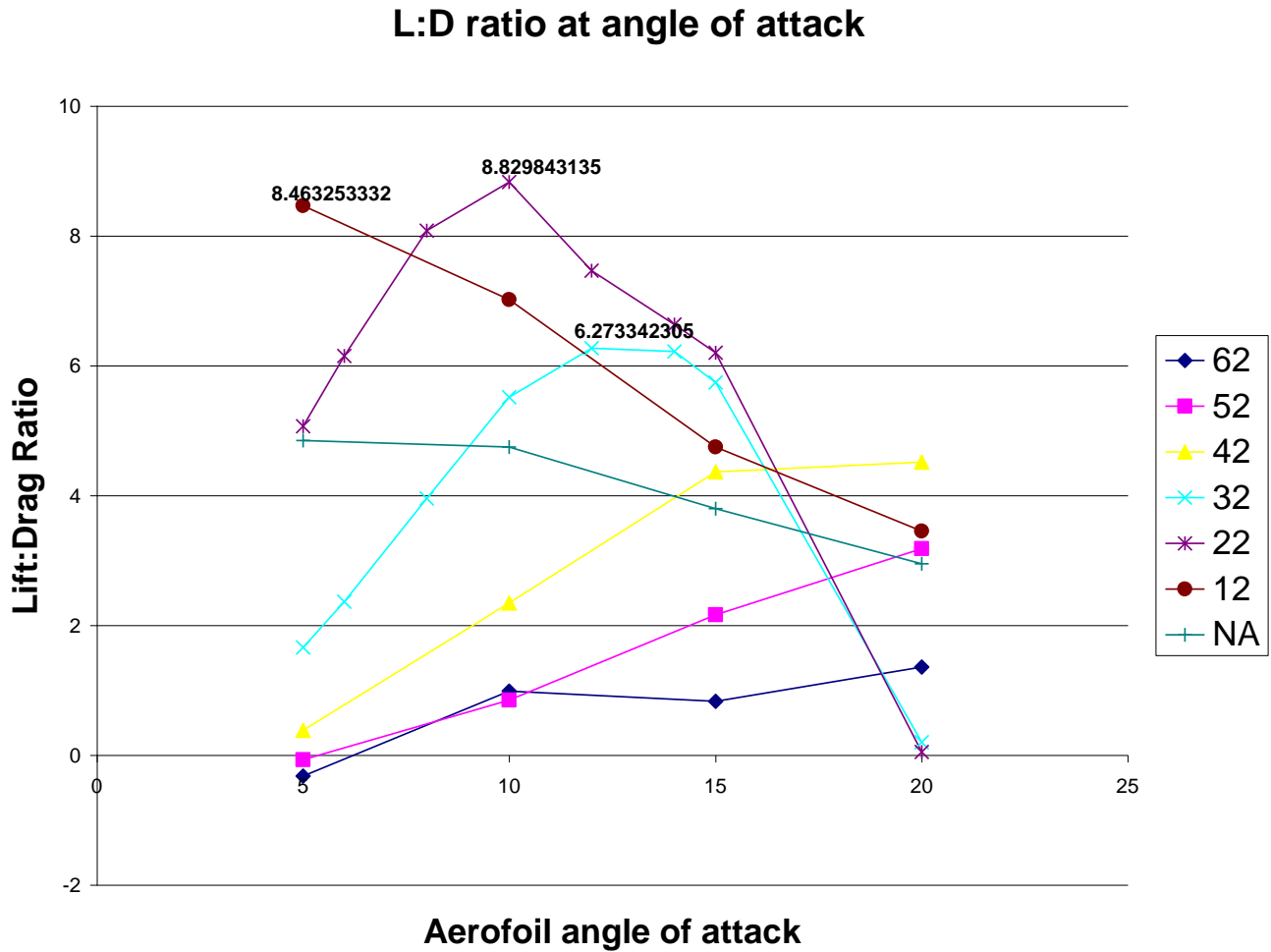
L:D ratio at angle of attack

Figure 15 – Lift and drag ratios as a function of angle of attack α for Ø_{pd} angles and for no propatagium.

The L:D ratios are highest for 12°, 22° and 32° with 32° have a high average ratio between an angle of attack of 10° and 15°. These results were done at a higher Reynolds number than those in Wilkinson's wind tunnel tests, using Bramwell and Whitefield chord lengths and free stream velocity.

The lower L:D ratios require more power. This supports the extra drag involved which reduced the L:D ratio initially. The weaknesses with the models are the discrepancies with the drag forces produced. This problem exists with Fluent and Java Foil.
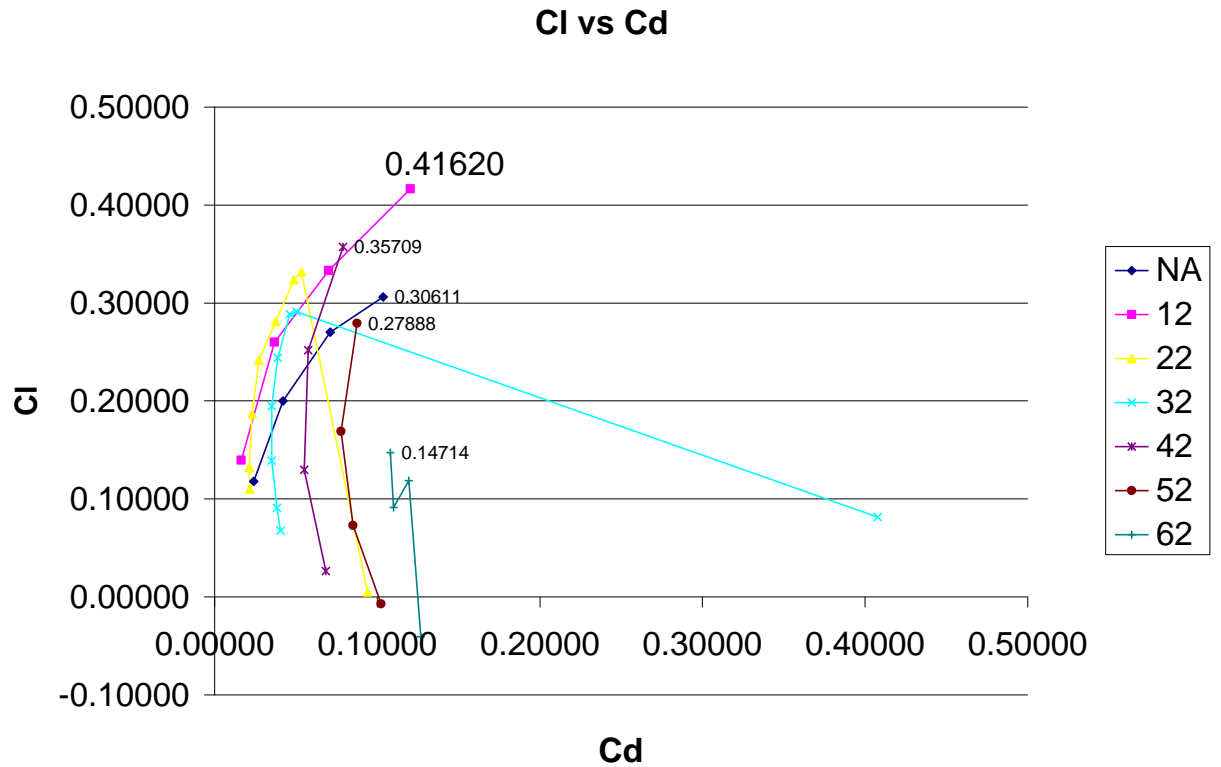
Figure 16 – Lift coefficients as a function of drag coefficients for Ø$_{pd}$ angles and for no propatagium.

The wing profile with a 32° propatagium deflection showed an acute increase in drag in relation to lift as shown in figure 16. This is because of the abrupt profile drag from a high increase in the angle of attack past the optimal lift. It could be used for a non-bone breaking landing. This drag is also used on aircrafts during landing where rear wing ailerons are deflected upwards in order to increase drag and induce breaking.

Powered flight requirements
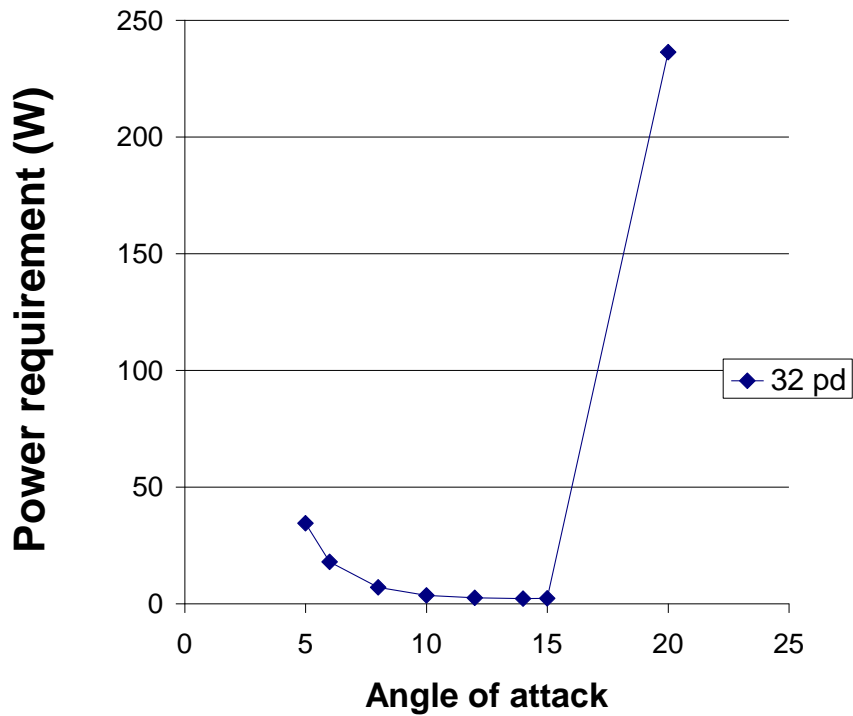
*Figure 17 shows the dramatic power requirement created from the drag at high angles of attack.*

The power requirement using the stall speed shows that the angle of attack would not very often exceed 15° as it would exhaust the creature.

With the increased power required for flight at angles of attack above 15°, it would be difficult for the creature to maintain sustained flight.
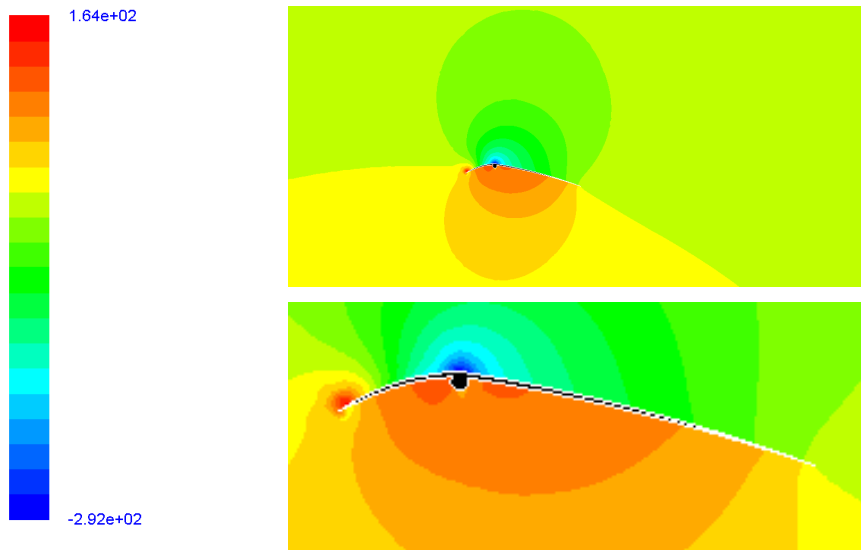
Figure 18 – Static pressure contours show the high pressure at the front flap and before and after the round spar for 32° pd deflection at 14° angle of attack

These models were taken from the angle of attack providing the optimum lift at its propatagium deflection. Figure 18 shows a build up of pressure on the leading edge and figure 19 shows evidence of the turbulent energy passing over the wing suggesting the absence of the bound vortices to the wings trailing edge. The loss of lift shows that the reverse vortex has been shed at angles of attack past 14°, giving the reason for the drop in the L:D ratio in figure 14 past 14°angle of attack.
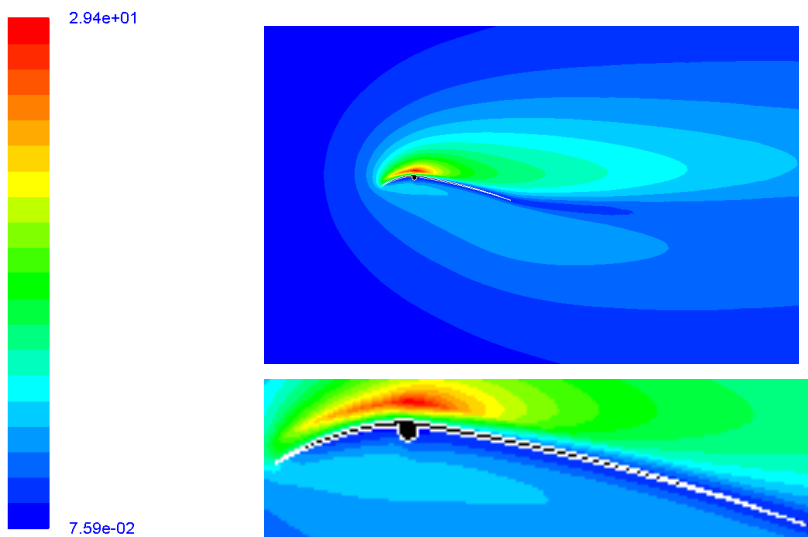
Figure 19 – Turbulence Kinetic Energy m²s⁻² for 32° pd deflection at 14° angle of attack

Modelling of the transition on the upper layer was possible using Java Foil table data and can be compared to the Fluent contour models. Java Foil gives a reading of 0.245 x/c for Transitional Upper (TU), which is the length along the chord at which the transition occurs on the upper surface on the wing. This agrees with the contours on Figure 18. Figure 20 was constructed from the output data values available in a table form from Java Foil, to show the lift coefficient as a function of location of the transition and separation on the wing. These shows were the flow alters to a turbulent nature.

Java Foil location of transition and separation for lift at a reynolds number of 120000
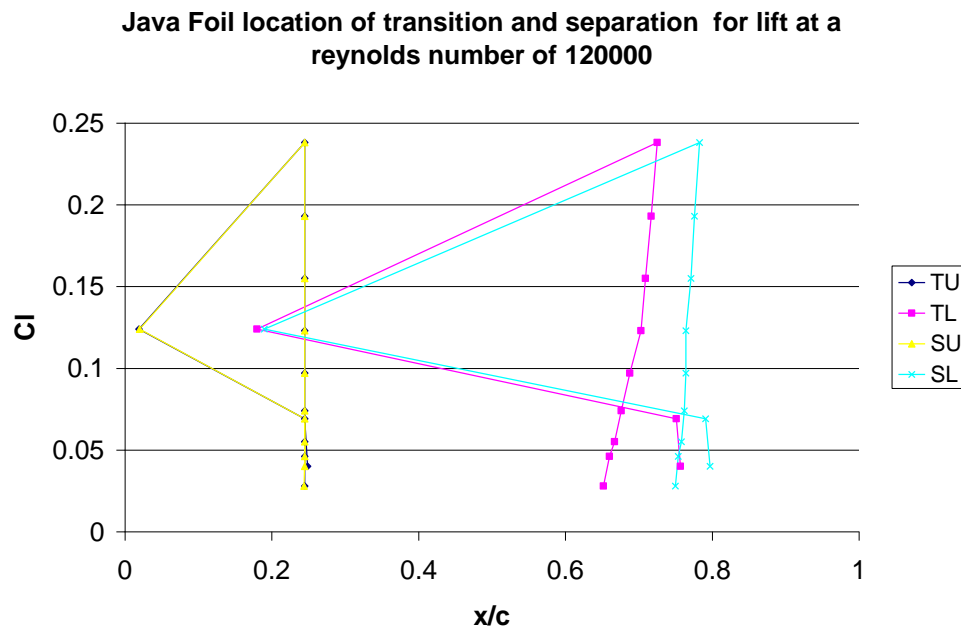
Figure 20 – Lift coefficient as a function of transition and separation location along 1m chord

The lower transitional distance profile lags the upper transitional distance profile. Separation should be close to the trailing edge and move forward slowly as maximum lift is reached. Turbulators are used to adjust the boundary layer behaviour to suit the required characteristics for a wing.
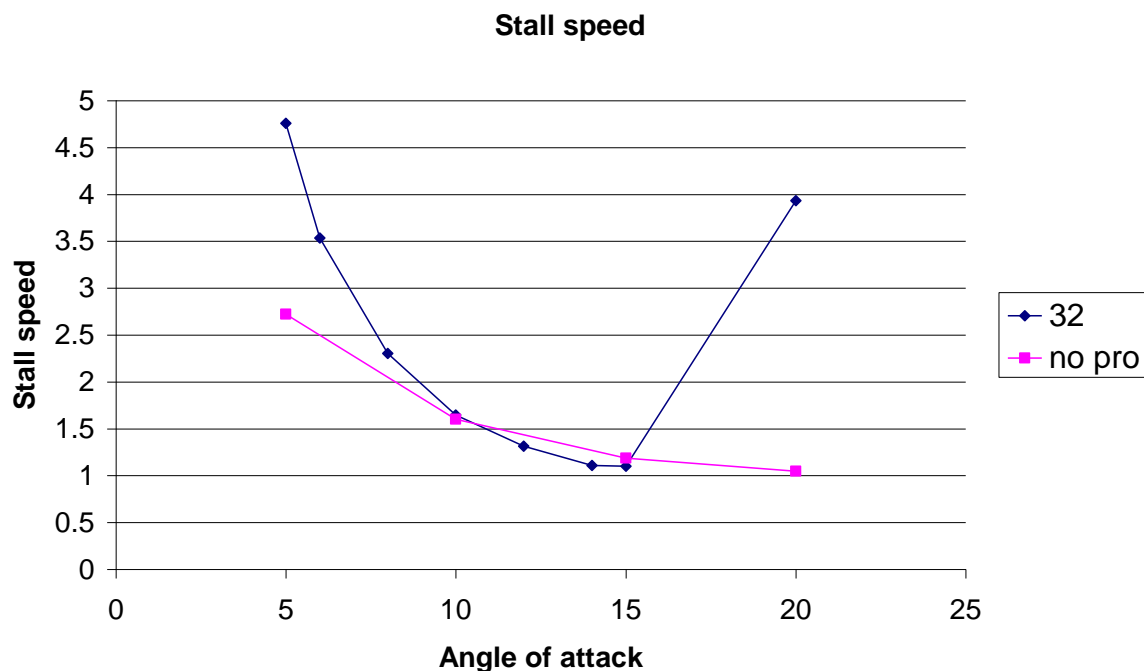
Stall speed

Figure 21 - Stall speed at varied angles of attack

Between the angles of attack of 10° and 15° the stall speed drops below that without the propatagium showing the ability to stay in the air at slower speeds. This would be extremely useful for such manoeuvres as feeding dynamics involving high speed descent at speeds of 15m s-1 down to speeds approaching 1.5 m s-1. The actual speed from feeding in water taking into account the drag produced from head and neck immersion. Hazelhurst and Rayner (1991) consider wing structure would prohibit full immersion and other researchers believe their long necks enabled them to scoop fish out of the water. Ground effects would also have to be taken into account for a full analysis.

Ground effect is an alteration in air flow around the wing caused by the interaction of vortices bound to the wing and shed in the wake reflecting on a close plane or surface Rayner (1991). This has the effect of reducing transport cost by up to 15% and mechanical power required by as much as 35%. Since the majority of pterosaur fossils have been located in areas of water sediment, researchers believe that their main diet was marine life, involving foraging over water. Therefore, it is likely that ground effect would have influenced their flight dynamics. Rayner and Thomas (1991) indicate that even when an animal is several wing spans distant from the surface, ground effect may still come in to play. The high aspect wing is a feature of animals using ground effect.   In Hazelhurst and Rayner's (1991) appraisal of Pterosaur wing shape, they present the theory of below average loading and above average aspect compared to the avian average.   The low loading from large wing surface area and low body mass is conducive to low speed and maneuverability unsuited to flying in cluttered environments. By adjusting the orientation of the pteroid to

broaden the wing, wing aspect is reduced. This has the effect of increased power at a low speed and would aid take off from the ground.

In the 2d and 3d modeling, ground effect was not considered. It may also be worth noting that in Wilkinson's wind tunnel tests, results could have been disrupted by the close proximity of the tunnel sides (Rayner 1991) The software used showed a different angle to look at the complete model. This helped while researching all the variables.
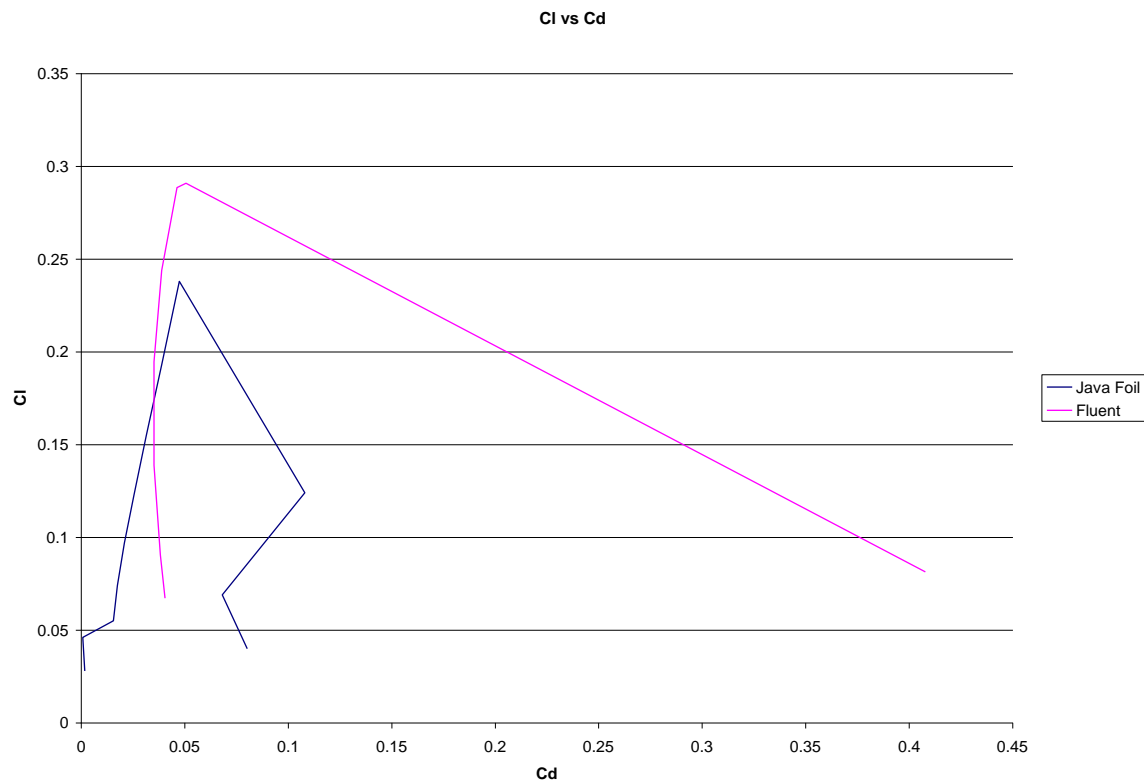

Figure 22 – Comparing lift and drag coefficient profile for same the 32° propatagium deflection model

DISCUSSION

A combination of factors in the morphology of pterosaurs resulted in their efficient flying techniques for over 140 million years. In the later larger species, these theories could be summarised:

- Small man sized body in comparison to wing spans in excess of 10 metres.
- Pneumatic bone structure reduced overall weight resulting in low wing loading conducive to low flight speeds and increased manoeuvrability.
- Notches found in the shoulder joint thought to enable 'locking' and add wing stability.

- A wing membrane as thin as 0.5mm thick, reinforced with actinofibrils to provide integrity and strength with soft tissue containing muscle, blood and neural networks.
- Brain control areas three fold larger than those of an average avian network. i.e. Well equipped to react to the smallest changes in external conditions, adding to flight control and agility.
- Theories that the large head crest apparent in some species could also have acted as a forward rudder to aid yaw. (see figure 21)
- The added advantage of a forewing or front aileron adjusted in orientation by the pteroid bone to impact on lift/drag forces.

With such a long wing for body size, the ability to furl the wings when on the ground would have enabled quadrupedal stance. This is now acknowledged by most researchers to account for the pteroid bone being positioned in a medial lie as it would have been flexed when wings were folded.
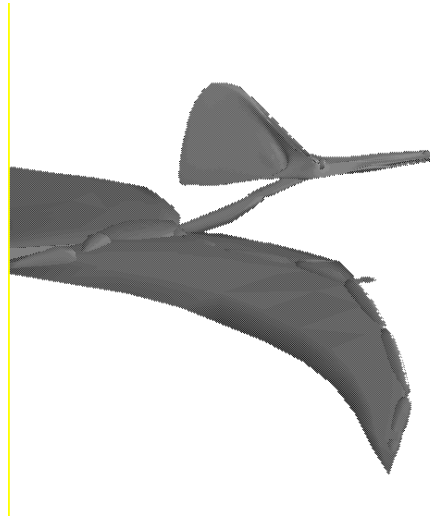

Figure 23– Large head crest on Studio Max model

Results from the 2d modelling support Wilkinsons theory but the angles of attack vary and this could be due to interaction of vortices with the wall.

Javafoil does not model laminar separation bubbles and flow separation, which leads to incorrect results if either occur. At stall, flow separation occurs and is modelled to some extent by empirical corrections, so that maximum lift can be predicted for normal aerofoils.

In any analysis of aerodynamics beyond the point of stall the results will be quite inaccurate. Numerical methods of calculation similar to Java Foil include Eppler code (PROFIL) and The Drela code (XFOIL) not to be confused as they are predecessors of Java Foil and agree astonishingly well with physical models, if the Reynolds numbers exceed 500,000. This is associated with the inviscid viscous model which analyses the flow without friction. Using a high Reynolds number creates a relative high free stream velocity at which point friction is negligible.
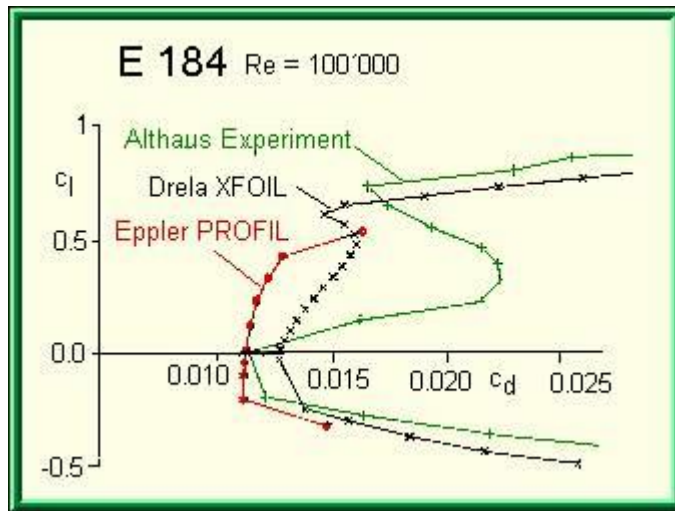
Figure 24 - Example of lift and drag coefficient plot of numerical models against experimental results from Java Foil website

The use of a higher Reynolds number may also have helped to minimise discrepancies as well as looking at speeds of descent for feeding.

The extreme angle of propatagium deflection does not allow smooth flow under the wing. In addition, it increases the drag and the spar disrupts the flow further.

Figure 15 showed that with no propatagium there was an increased drag. This is associated with airflow meeting the diameter of the spar. Contact with this larger area causes increased drag.

A similar effect can be seen with a propatagium deflected at angles of 42° and above. Here, the higher deflection creates a larger contact area on the upper surface of the propatagium influencing greater drag forces. This increased drag would increase stall and reduce flight speed. Energy requirements as a result of the increased stall and the need for flapping to sustain flight, would be higher. However, an ability to increase stall in this way would facilitate landing and reducing height for plucking fish out of water, as previously mentioned.

With a propatagium deflected between 12° and 32° optimal lift was achieved at an angle of attack between 10° and 15°. At lower angles of attack there was a poorer performance in lift for all models except those with no propotagium and with a propotagium deflected at 12°. The latter somewhat surprising result may be attributed to the camber of the propatagium lying above the spar diameter thereby aiding lift.

Overall it supports the high lift function of a model with a propatagium. The presence of a front wing flap increases wing area as shown by Hazelhurst and Rayner (1992) in appendix (i. An increased wing area results in lower wing loading and improved lift, aiding take-off and reducing the need for running at speed or flapping. At varying deflections the propatagium affects both lift and

drag enabling adjustment to suit air velocity and different manoeuvres, aiding flight control.

CONCLUSION

The results show that the propatagium shared similarities with turbulators, which are found on the leading edge of modern aircraft airfoils, these help to reduce stall speeds and improve stability in flight manoeuvres. The Upper Transitional distance along the chord dictates the position of these turbulators.

Any results analysing the flight characteristics in 2d are not a final result because the induced drag at the tips of wings was not taken into account. A 3d model would be more suitable for such analysis. Although this wing tip turbulence or induced drag would have added extra drag, it does not diminish the effectiveness of the front edge wing flap created by the antero-ventral orientation of the pteroid bone. With a broad front wing flap at higher angles of attack the highest L:D ratios were achieved. This could be because of the minimal shock conditions associated with such a wing orientation, these reduce the amount of incidence force applied as in a turbine blade or pelton wheel cup.

OVERVIEW

The whole project took approximately 300 hours to complete. This involved:

Thorough scrutiny of available research accessed mainly through electronic journals.

- Selecting suitable software for both 2d and 3d modelling

- Learning to use unfamiliar software programs

- Creating the models and adapting parameters

- Interpreting and analysing the results

- Writing up the report

Although the project took much longer than expected, enough results were obtained to draw a positive conclusion which agreed with Wilkinson's physical model. The process has provided a positive learning experience and a possibility for future development. Further work on the 3d modelling would be a natural progression.

REFERENCES

Bramwell, C.D. and Whitfield, G.R. (1974) Biomechanics of Pteranodon. Phil. Trans. R. Soc. Lond. B. Boilogical Sciences Vol 267 No 890 pp 503-581

Chatterjee, S. and Templin, R.J. (2004) Posture, locomotion and paleoecology of pterosaurs. Geological Society of America Special Paper 376

Gray, J. (1968) Animal Locomotion. Weidenfield and Nicolson, London p 479

Hazelhurst, G.A. and Rayner, M.V. (1992) Flight characteristics of Triassic and Jurassic Pterosauris: an appraisal based on wing shape. Paleobiology Vol 18 No 4 pp 447-463

Marks, P. (2005) Found: the flying lizards' missing lift. New Scientist October

Martill, D.M. and Unwin, D.M. (1989) Exceptionally well preserved pterosaur wing membrane from the Cretaceous of Brazil. Nature Vol 340 pp 138-140

Padian, K. (1983) A functional analysis of flying and walking in pterosaurs. Paleobiology, Vol 9 No3 pp 218-239

Rayner, J.M.V. (1991) On the aerodynamics of animal flight in ground effect. Phil. Trans. R. Soc. Lond. Vol 334 pp 119-128

Rayner, J.M.V. and Thomas, A.L.R. (1991) On the vortex wake of an animal flying in a confined volume. Phil. Trans: Biological Sciences Vol 334 No 1269 pp 107-117

Stein, R.S. (1975) Dynamic analysis of Pteranodon Ingens: a reptilian adaptation to flight. J. of Paleontology, Vol 49 No3 pp 534-548

Tytell, E. (2006) Pterosaurs Ptake off. Journal of Experimental Biology Vol 209

Unwin, D.M. (2003) Smart-winged pterosaurs. Nature Vol 425 pp 910-911

Unwin, D.M. and Bakhurina, N.N. (2002) Sordes pilosus and the nature of the pterosaur flight apparatus. Nature Vol 371 pp 62-64

Unwin, D.M., Frey, E., Martill, D.M., Clarke, J.B. and Reiss, J. (1996) On the nature of the pteroid in pterosaurs. Proc. R. Soc. Lon. B Vol 263 pp 45-52

Wilkinson, M.T., Unwin, D.M. and Ellington, C.P. (2005) High lift function of the pteroid bone and forewing of pterosaurs. Proc. R. Soc. B doi:10.1098/rspb.2005.3278

Witmer, L.M., Chatterjee, S., Franzosa, J. and Rowe, T. (2003) Neuroanatomy of flying reptiles and implications for flight, posture and behaviour. Nature Vol 425 pp950-953

Witton, M. (2007) Titans of the skies: azhdarchid pterosaurs. Geology Today Vol 23 No 1 pp 33-38

i)

Species and reference	Mass (kg)	Wing span	Wing area m²	
Campylognathoides zitteli SMNS	0.498	1.614	1 2 3	0.154 0.213 0.285
R. muensteri SMF R4128 Gross 1937	0.186	1.048	1 2 3	0.064 0.087 0.109
Nyctosaurus gracilis	1.87	2.72	1	0.451
Dsungaripterus weii	4.70	3.24	1	0.816
Pteranodon	16.60	6.95	1 3	2.08 4.62

Dimensions of reconstructed pterosaurs. Adapted from Hazelhurst and Rayner (1992) p 455. Wing area models: 1 – leg free of membrane; 2 – wing membrane extended to knee; 3 – wing membrane extended to ankle.
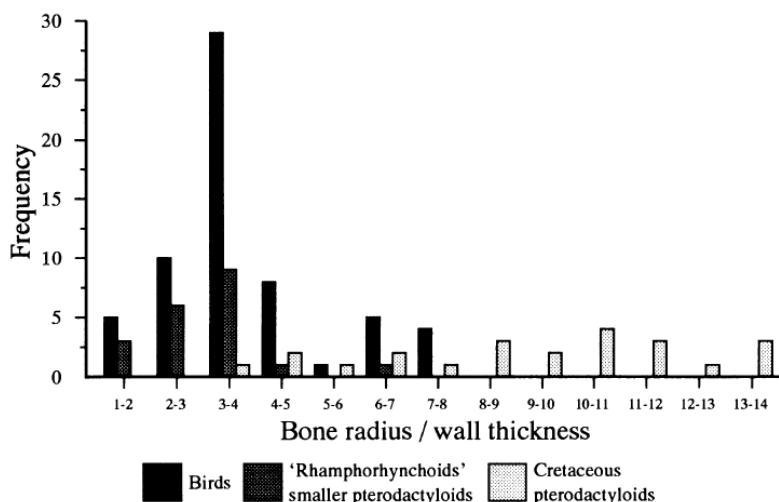
ii)

FIGURE 2. Distribution of bone-wall thickness in pterosaurs and birds. Data for birds are from Currey and Alexander (1985). The measurements for pterosaurs are from long bones and wing phalanges. The pterosaurs are divided into two categories: the "rhamphorhynchoid" and smaller pterodactyloid category includes pterosaurs similar in size to extant birds, and the giant Cretaceous pterodactyloid category covers the larger species. Some Cretaceous pterodactyloids have extremely thin wing bones, suggesting that it is inappropriate to use avian density for these animals.